

long short-term memory (LSTM) architecture was adopted. Its memory cells and gating mechanisms mitigate vanishing gradient issues and enhance training stability. The LSTM model demonstrated high accuracy in forecasting energy demand, enabling precise prediction of future power consumption based on historical data. Incorporating external features, such as weather conditions and diurnal patterns, further improved forecast reliability, supporting optimized resource allocation and adaptive control strategies.

To identify the primary factors influencing system energy consumption, we selected eight key input variables based on domain knowledge and sensor availability. These variables include chilled water inlet temperature (T_{in_cw}), chilled water outlet temperature (T_{out_cw}), chilled water flow rate (Q_{cw}), ambient wet bulb temperature (T_{wb}), cooling water temperature setpoint ($T_{set_cooling}$), cooling water inlet temperature ($T_{in_cooling}$), cooling water outlet temperature ($T_{out_cooling}$), and cooling water flow rate ($Q_{cooling}$). To enable precise characterization of energy distribution across the system, the output layer was designed to model the power consumption of four major equipment groups separately: chillers ($P_{chillers}$), cooling towers ($P_{cooling_towers}$), chilled water pumps ($P_{chilled_water_pump}$), and cooling water pumps ($P_{cooling_water_pump}$). As shown in Fig. 2, these output variables represent the total power usage of each subsystem. For consistency, measurement units were standardized as follows: temperature in degrees Celsius ($^{\circ}C$), power in refrigeration tons, and flow rate in gallons per minute (GPM). These eight input features and four output variables served as the main training variables for the RNN-based predictive model. To ensure robustness, the system was tested under various operating conditions, including changes in water flow rates, chilled water setpoints, and cooling tower approach values. High-resolution sensors captured system dynamics, yielding 864,000 raw samples. After noise removal and data cleaning, the dataset was aggregated into 28,800 high-quality samples for training, validation, and benchmarking, providing a solid foundation for data-driven energy optimization. Ultimately, this workflow produced a robust surrogate model that accurately characterizes the system's energy performance across different operating conditions.

Hybrid LSTM-Bayesian Optimization of Power Consumption

To enhance optimization capabilities, the LSTM predictive model was integrated into a Bayesian optimization framework. This approach enables systematic exploration of operational parameters to minimize energy use while ensuring system reliability and thermal comfort. Bayesian optimization is well-suited for optimizing expensive black-box functions by using a probabilistic surrogate model to guide the search toward promising regions. Traditional Gaussian process regression (GPR) provides useful uncertainty estimates but scales poorly with large datasets due to its $O(n^3)$ complexity, making it less suitable for high-resolution time-series data. By contrast, LSTM models train efficiently with graphic processing unit (GPU) acceleration and can handle large sequential datasets. Replacing GPR with an LSTM-based surrogate improves both accuracy and scalability while preserving the sample efficiency of Bayesian optimization. This hybrid LSTM-Bayesian optimization framework enables simulation across a wide range of operating conditions and offers robust data-driven guidance for energy performance optimization. As shown in Fig. 3, the search input space, defined by practical ranges of temperatures, flow rates, and setpoints, allows the system to identify optimal operating conditions automatically through iterative, intelligent sampling.

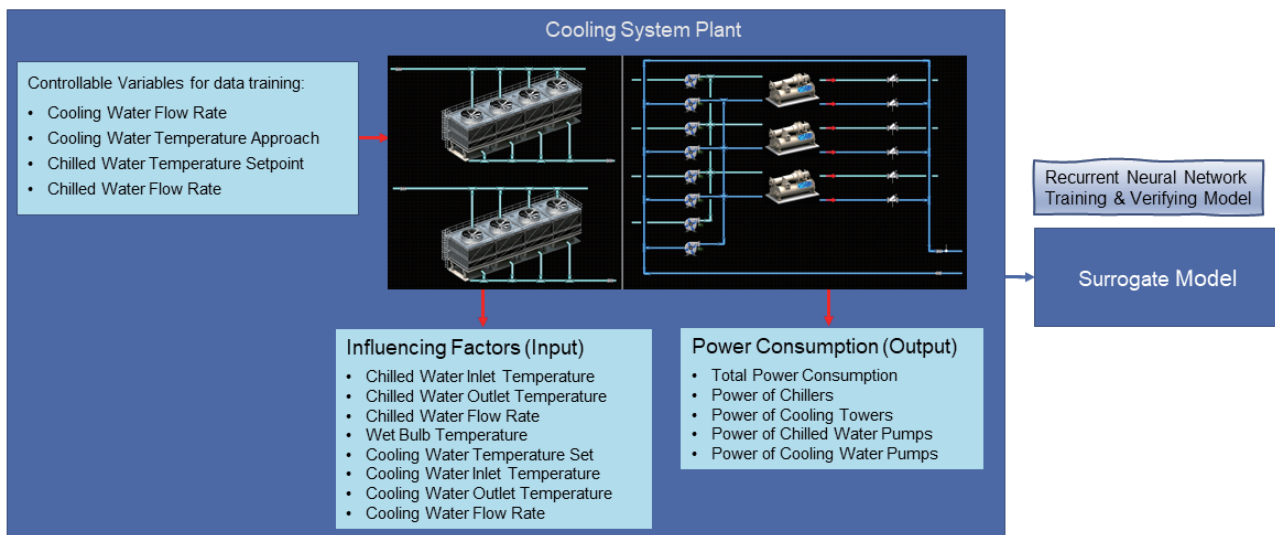


Fig. 2: Schematic diagram of the training model for the cooling tower and chilled water systems. [Reproduced from Ref. 4]

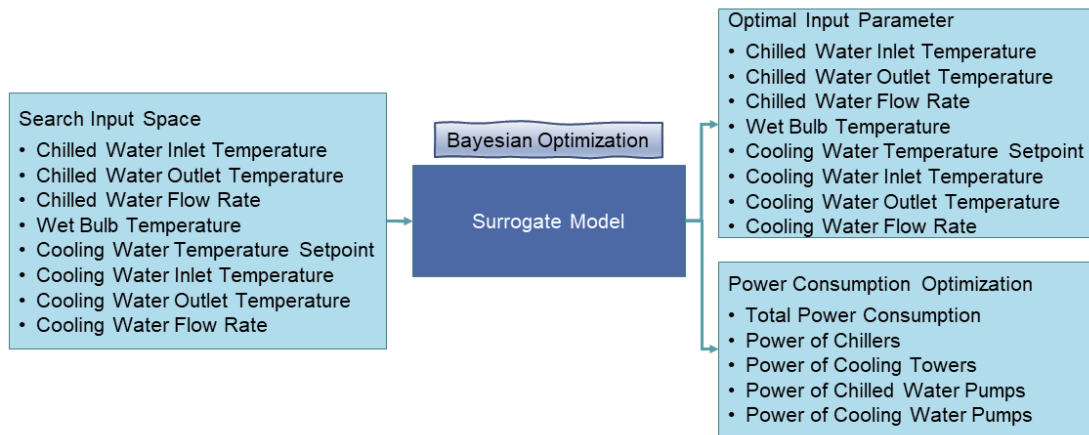


Fig. 3: Schematic diagram of the surrogate model used in Bayesian optimization. [Reproduced from Ref. 4]

Verification of Real-World Operational Adjustments

To validate the predictive model and assess real-world operational impacts, a series of parametric analyses were conducted, focusing on key environmental and control parameters within the cooling system.

Effect of Wet Bulb Temperature on System Power Consumption

The wet bulb temperature represents the thermodynamic lower limit for the outlet temperature of evaporative cooling towers. Regardless of how much cooling capacity is available, the outlet temperature cannot drop below the ambient wet bulb temperature. For efficient operation, the outlet temperature is therefore controlled at the wet bulb temperature plus a fixed 2 °C approach. With the cooling water inlet temperature fixed at 32 °C, the simulation results in **Table 1** show that decreasing wet bulb temperatures reduces chiller power consumption.

By contrast, when cooling tower power rises, pump power remains unchanged due to constant flow rates. As a result, total system power decreases with wet bulb temperature decreases, highlighting the chiller’s dominant impact on overall energy use.

Table 1: Effect of wet bulb temperature variation on power consumption.

$T_{set_cooling}$	T_{wb}	$P_{chillers}$	$P_{cooling\ towers}$	P_{total}
30.0	28.1	1098	99	1398
29.0	27.1	1082	105	1392
28.1	26.1	1060	123	1388
27.0	25.1	1041	132	1377
26.0	24.1	1034	136	1371

Impact of the Cooling Tower Approach on Energy Performance

Although ambient wet bulb temperature cannot be controlled, the approach temperature, defined as the difference between the cooling tower outlet setpoint and the wet bulb temperature, can be adjusted through design and operation. With the cooling water inlet temperature fixed at 32 °C, **Table 2** (see next page) shows that decreasing the approach reduces chiller power consumption while increasing cooling tower power, with the total system energy use still dominated by the chiller. Thus, minimizing the approach temperature is an effective design strategy for improving energy efficiency. This modeling indicates that reducing the approach from 4.0 to 2.0 °C can yield about 1.5% of energy savings. This result supports ongoing hardware upgrades aimed at improving heat-rejection capacity and enabling smaller approach values for better overall system performance. If extrapolation remains valid, an approach of approximately 1.5 °C could potentially deliver up to 1.93% of energy savings.

Table 2: Effect of variations in the cooling tower approach on power consumption.

$T_{set_cooling} - T_{wb}$	$T_{out_cooling}$	$P_{chillers}$	$P_{cooling\ towers}$	P_{total}	Efficiency
4.0	29.1	1094	99	1394	0
3.5	28.5	1081	102	1391	0.22%
3.0	28.0	1066	121	1387	0.50%
2.5	27.6	1053	130	1383	0.79%
2.0	27.1	1041	132	1373	1.50%
1.5	26.6	1030	136	1367	1.93%

Influence of Cooling Water Flow Rate

The cooling water flow rate was reduced from 9000 GPM to 6500 GPM, remaining within the safe range required to avoid triggering chiller protection. As shown in **Table 3**, lowering the flow rate significantly reduces cooling water pump power, while chiller and cooling tower power remain largely unchanged. This results in a total energy reduction of 2.78%. Therefore, operating at the minimum flow rate that still meets the chiller’s base-load requirements is an effective strategy for improving system efficiency.

Table 3: Effect of variations in the cooling tower flow rate on power consumption.

$T_{cooling\ flow}$	$P_{cooling\ pumps}$	$P_{chillers}$	$P_{cooling\ towers}$	P_{total}	Efficiency
9000	155	1252	129	1585	0
8500	141	1254	127	1575	0.63%
8000	134	1256	130	1572	0.82%
7500	130	1253	135	1567	1.14%
7000	126	1247	138	1558	1.70%
6500	121	1238	134	1541	2.78%

Several practical power-saving measures were evaluated to quantify their potential impact on overall system efficiency. As summarized in **Table 4**, reducing the cooling tower approach temperature yields energy savings of 1.5–1.93%, while lowering the cooling water flow rate provides a 2.78% reduction in total power consumption. Further improvements can be achieved through system-level enhancements, such as using return chilled water to cool deionized water loops (approximately 1.6% of efficiency gain), and installing pressure-independent control valves, which contribute additional savings from both chillers and chilled water pumps. Here, η represents energy efficiency. Adjusting the chiller setpoint also offers substantial energy-saving potential. Depending on the operational scenario, total efficiency improvements can exceed 5.88%, with further gains possible when combined with optimized pump operation, flow control, and temperature management. Collectively, these measures provide a comprehensive pathway for improving system-wide energy performance and support future optimization efforts. (Reported by Zong-Da Tsai)

Table 4: Quantitative evaluation of AI-driven power-saving effects.

Power-saving Measures	Efficiency (%)
Approach Variation	1.5–1.93
Cooling Water Flow Variation	2.78
Deionized Water Cooled with Return Chilled Water (600 GPM)	$\eta_{chillers} + 1.6$
Pressure Independent Control Valve (~1200 GPM)	$\eta_{chillers} + \eta_{chilled\ pump-1} + \eta_{chilled\ pump-2}$
Chiller Setpoint	$\eta_{chillers}$
	5.88 + η_{more}

References

1. L. Xie, K. Shan, H. Tang, S. Wang, Adv. Appl. Energy **18**, 100220 (2025).
2. E. Dulce-Chamorro, F. J. Martinez-de-Pison, J. Build. Eng. **43**, 102839 (2021).
3. S. Xing, J. Zhang, S. Li, J. Gao, H. Guan, Appl. Energy **376**, 124208 (2024).
4. Z. D. Tsai, C. S. Chen, MEDSI’**25**, 321 (2025).